NATIONAL ADVISORY COMMITTEE FOR AERONAUTICS

TECHNICAL NOTE

No. 1388

PERFORMANCE OF AN AXIAL-FLOW COMPRESSOR ROTOR DESIGNED FOR A PITCH-SECTION LIFT COEFFICIENT OF 1.20

By L. Joseph Herrig and Seymour M. Bogdonoff

Langley Memorial Aeronautical Laboratory
Langley Field, Va.

Washington
July 1947

NATIONAL ADVISORY COMMITTEE FOR AERONAUTICS

TECHNICAL NOTE NO. 1388

PERFORMANCE OF AN AXIAL-FLOW COMPRESSOR ROTOR DESIGNED FOR A PITCH-SECTION LIFT COEFFICIENT OF 1.20

By L. Joseph Herrig and Seymour M. Bogdonoff

SUMMARY

The performance of a set of axial-flow fan and compressor rotor blades having high design loading was studied in a low-speed test blower. The tests were made without entrance vanes or stators. The pitch-section lift coefficient at the design condition was 1.20 at a solidity of 1.0 as compared with the highest value of 0.99 reported in NACA TN No. 1201.

The increase in design loading over that of previous tests gave increased pressure rise per stage while a peak efficiency of 96 percent and a good operating range were maintained. Deviation of peak efficiency from the design point indicated that optimum performance would be obtained by using sections of higher camber at lower angles of attack to fulfill the design conditions. At a solidity of 1.0, an average design lift coefficient of at least 1.2 can be used with high efficiency, and maximum lift coefficients above 1.4 are indicated. Extreme leading-edge roughness caused a 3.5-percent decrease in efficiency and an 11-percent decrease in static-pressure rise at design conditions.

INTRODUCTION

An investigation of a systematic series of rotor blades operating with average lift coefficients from 0.3 to 0.99 is reported in reference 1. That investigation showed that high design loadings give high pressure rise per stage while high efficiency and wide operating range are maintained. The trends of the lift and pressure-rise curves indicate, moreover, that even higher design loadings might be used. The investigation of reference 1 is therefore extended in the present paper to include a blade of higher loading than those previously reported. The pitch-section lift coefficient of the present blade at the design condition is 1.20 at a solidity of 1.0 compared with the value of 0.99 previously attained at the same solidity. The performance of the present blade was compared with that of the most highly loaded blade previously tested. The tests were made in a single-stage test blower at the Langley Memorial Aeronautical Laboratory of the National Advisory Committee for Aeronautics.

SYMBOLS

A	annulus area, square feet
c_l	blade-section lift coefficient
c_p	specific heat of air at constant pressure, foot pounds per slug per $^{\circ}F$
D	diameter, feet
H	total pressure, pounds per square foot
ΔH	weighted-average total-pressure rise, pounds per square foot
n	rotor speed, revolutions per second
p	static pressure, pounds per square foot
Δp	static-pressure rise, pounds per square foot
Q	quantity flow, cubic feet per second
q	dynamic pressure, pounds per square foot
T	temperature, $^{\circ}F$ absolute
U	rotational velocity of rotor blade element at any radius, feet per second
V	velocity of air relative to casing, feet per second
W	velocity of air relative to rotor, feet per second
Δw	change in tangential velocity, feet per second (measured parallel to blade row)
α	angle between effective entering air and chord line, degrees
α_m	angle between mean air and chord line, degrees
β	stagger angle, degrees (angle of effective entering air measured from axial direction)
β_m	mean stagger angle, degrees (angle of mean air measured from axial direction)

δ ratio of change in tangential velocity, Δw, to axial velocity, V_a

η adiabatic rotor efficiency evaluated from surveys one-half chord upstream and one-half chord downstream from rotor

$$\eta = \frac{\int^A c_p\left(\rho_2 V_{a_2} T_{s_{2_{ad}}} - \rho_1 V_{a_1} T_{s_1}\right) dA}{\int^A U\left(\rho_2 V_{a_2} \Delta w\right) dA}$$

θ effective angle through which air is turned relative to rotor, degrees

ρ mass density, slugs per cubic foot

ϕ angle through which air is turned relative to casing, degrees

σ solidity (blade chord divided by gap between blades or number of blades times chord divided by circumference)

$\frac{\Delta p}{q_m}$ section static-pressure-rise coefficient based on mean dynamic pressure

$\frac{p - p_{atm}}{\frac{1}{2}\rho U_t^2}$ local static-pressure coefficient

$\frac{\Delta H}{\frac{1}{2}\rho U_t^2}$ fan total-pressure-rise coefficient

$\frac{H - p_{atm}}{\frac{1}{2}\rho U_t^2}$ local total-pressure coefficient

$\frac{Q}{nD_t^3}$ quantity coefficient

Subscripts:

1 entering rotor

2 leaving rotor

a	axial direction
ad	adiabatic
atm	atmospheric conditions
m	mean-air conditions (one-half vector sum of entering and leaving values)
p	pitch section (midway between root and tip sections)
s	stagnation
t	tip

APPARATUS AND PROCEDURE

The tests were made in the single-stage test blower described in reference 1. The test section had a constant area through the blades with an outside diameter of 27.82 inches and an inside diameter of 21.82 inches. The blades were approximately 3 inches long with a constant blade chord of 3 inches. No entrance vanes or stators were used. Roughness was simulated by placing a strip of $\frac{1}{2}$-inch masking tape over each blade leading edge so that $\frac{1}{4}$ inch was on each surface. The test procedure was the same as that used in reference 1. The speed was held constant at 2000 rpm for all tests and the quantity flow was varied from the maximum obtainable to stall by throttling. No data were taken in the stalled condition. Surveys of yaw angle and static and total pressures were taken one-half chord upstream and downstream from the rotor for each test. All performance calculations were made from the data provided by the surveys. The Reynolds numbers for the tests varied from 300,000 to 500,000 and the Mach numbers varied from 0.20 to 0.26 based on blade chord and mean-air conditions relative to the rotor.

The blade design procedure for the present blade was the same as that for the blades described in reference 1; free-vortex-type flow was used and solidity of 1.0 at the pitch section and constant chord were maintained. A typical vector diagram is shown in figure 1. The high loading used, however, required profiles of higher camber than those reported in references 2 and 3. Since no cascade data were available for the higher loadings used, the design charts of reference 3 were extrapolated to give the profiles and angle settings; it is not known, therefore, whether the shapes of the pressure distribution curves were

optimum at the design condition. The blade designation is given in terms of loading as the design ratio of change in tangential velocity at the pitch section to the axial velocity; for the present blade $\delta = 0.875$ as compared with the previous highest value of 0.7. Design information for the blade is given in table I.

The clearance between the blade tips and the casing was 0.007 ± 0.002 inch. The gaps at the rotor surfaces, which were unsealed for the tests of the previous blades, were sealed with modeling clay for the tests of the present blade. The blade material was cast aluminum and the blade surfaces were not machined; the surface condition and profile accuracy, therefore, were somewhat inferior to those of the machined blades used in previous tests of this series. Sealing the gaps at the hub would tend to increase the efficiency while the poorer blade construction would tend to decrease efficiency. The results are believed to be comparable to those of reference 1 within the accuracy of the tests.

RESULTS AND DISCUSSION

The efficiency curve (fig. 2) shows that the peak efficiency of approximately 96 percent, which was reported for the 0.4, 0.6, and 0.7 blades in reference 1, was maintained for the 0.875 blade. The range of quantity coefficient for which high efficiency was obtained was also comparable to the range of the blades of reference 1.

The efficiency contours superimposed on the pitch-section-lift curves, which were originally presented for the previous blades in figure 7 of reference 1, have been redrawn to include the new data (fig. 3). These results show that high efficiency can be obtained with design lift coefficients above those used in reference 1 and indicate that perhaps even higher values might be used. It can be seen in figures 2 and 3, however, that the maximum efficiency for the 0.875 blade occurs at a condition of higher quantity flow and lower angle of attack than the design condition. Although the efficiency values reflect performance of the blade as a whole rather than individual sections, it is apparent that more nearly optimum performance would be obtained at the design condition if sections of higher camber were used at lower angles of attack to give the design turning angles. The point of maximum blade efficiency as well as the design point is indicated in all plots where possible.

Figures 4 and 5 give the lift and pressure-rise curves for the 0.875 blade compared with those for the 0.7 blade. For the design conditions, the pitch-section lift coefficient is 1.20 for the 0.875 blade and 0.99 for the 0.7 blade. If the point of maximum blade

efficiency is used in the comparison, the corresponding values are 1.10 and 0.99. The maximum lift coefficients at the pitch section are 1.30 and 1.19 for the two blades. Corresponding increases occurred in the pressure-rise coefficients. Calculation of lift coefficients near the root was difficult because of secondary flows, but it is estimated that the maximum lift coefficient there was about 1.45. The trend of higher lift and pressure-rise coefficients with higher camber has apparently been maintained. The static-pressure rise at design conditions was 94 percent of the ideal value calculated from measured stagger and turning angle, not including losses.

The fan total-pressure curves for the 0.875 and 0.7 blades are compared in figure 6. For an operating Mach number of 0.8 at the tip section, loadings comparable to those obtained in the tests, free-vortex-type diagrams with entrance vanes, and the diameter ratio of the test blower, calculations show that stage pressure ratios of the order of 1.4 can be obtained.

A comparison of the pitch-section turning angles for the 0.875 and 0.7 blades are presented in figure 7. In figures 8 to 10, surveys of turning angles, velocities, and pressures are shown. The turning angles of figure 8 show that, at the design condition, the measured values check the desired design angles to $\pm 1^{\circ}$ over the part of the blade not affected by the root and tip flows. Figures 9 and 10 show how closely the actual performance approached the constant axial velocity and constant-total-pressure increase along the blade for which the blade was designed. The root and tip effects are comparable to those found in reference 1.

Simulated blade roughness caused a decrease in efficiency of 3.5 percent and a decrease in turning angle of approximately 2° at the design condition (figs. 2 and 8). These decreases correspond to decreases of 11 percent in static-pressure rise and 10 percent in lift coefficient (figs. 4 and 5). These roughness effects appear to be no more severe than those encountered for blades of lower loading in reference 1.

CONCLUSIONS

Rotating tests of a compressor blade designed for an average lift coefficient of 1.20 showed that the increase in design loading over that of previous tests gave increased pressure rise per stage while a peak efficiency of 96 percent and a good operating range were maintained. Deviation of peak efficiency from the design point indicated that optimum performance would be obtained by using sections of higher

camber at lower angles of attack to fulfill the design conditions. At a solidity of 1.0, an average lift coefficient of at least 1.2 can be used with high efficiency, and maximum lift coefficients above 1.4 are indicated. Extreme leading-edge roughness caused a 3.5-percent decrease in efficiency and an 11-percent decrease in static-pressure rise at the design condition.

Langley Memorial Aeronautical Laboratory
National Advisory Committee for Aeronautics
Langley Field, Va., May 19, 1947

REFERENCES

1. Bogdonoff, Seymour M., and Herrig, L. Joseph: Performance of Axial-Flow Fan and Compressor Blades Designed for High Loadings. NACA TN No. 1201, 1946.

2. Bogdonoff, Seymour M., and Bogdonoff, Harriet E.: Blade Design Data for Axial-Flow Fans and Compressors. NACA ACR No. L5F07a, 1945.

3. Bogdonoff, Seymour M., and Hess, Eugene E.: Axial-Flow Fan and Compressor Blade Design Data at 52.5° Stagger and Further Verification of Cascade Data by Rotor Tests. NACA TN No. 1271, 1947.

TABLE I

BLADE DESIGN DETAILS

[Profiles and settings obtained by extrapolation from figure 14 of reference 3]

Section	β (deg)	θ (deg)	σ	Blower-blade section	α (deg)
Root	51.7	36.6	1.135	65-(20)10	21.0
Pitch	55.2	25.8	1.000	65-(16)10	18.0
Tip	58.2	18.5	0.892	65-(12)10	15.5

NATIONAL ADVISORY
COMMITTEE FOR AERONAUTICS

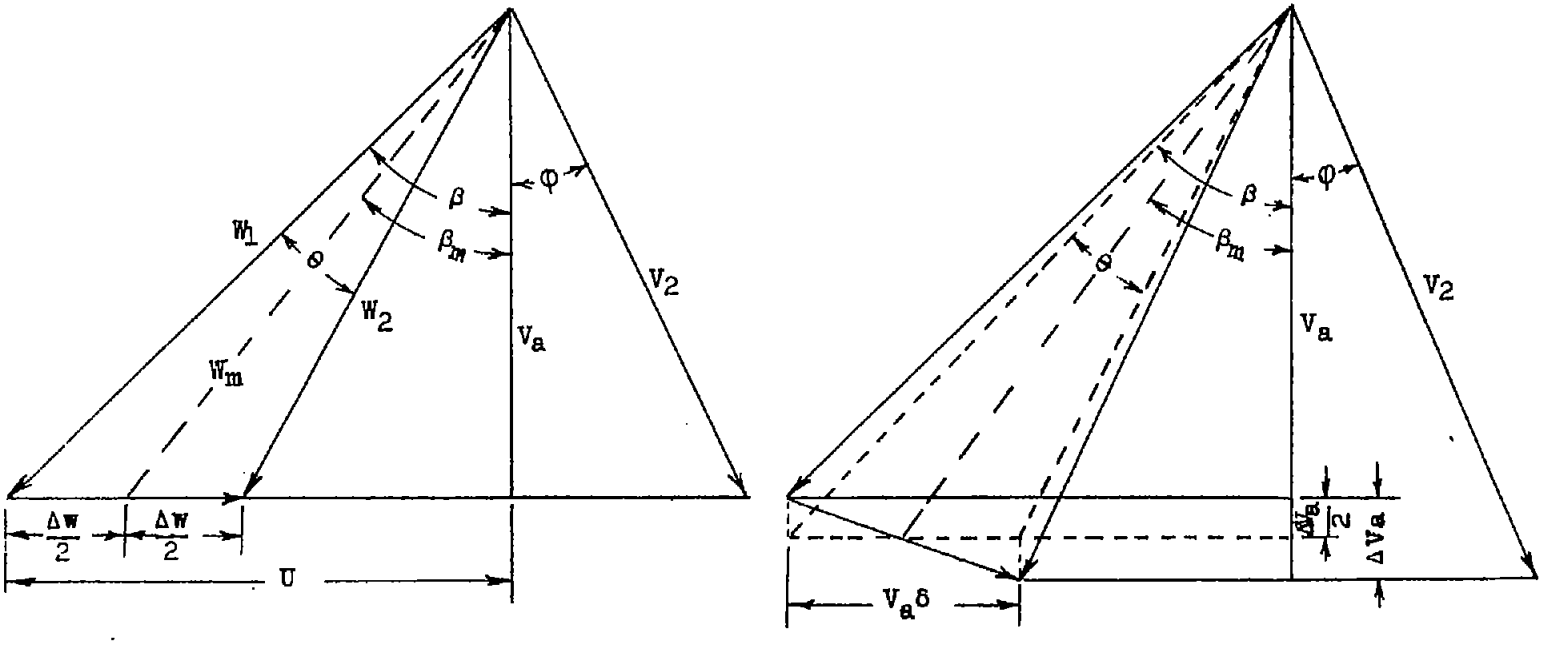

(a) Constant axial velocity.

(b) Varying axial velocity.

NATIONAL ADVISORY
COMMITTEE FOR AERONAUTICS

Figure 1.- Typical vector diagrams for axial-flow fans and compressors.

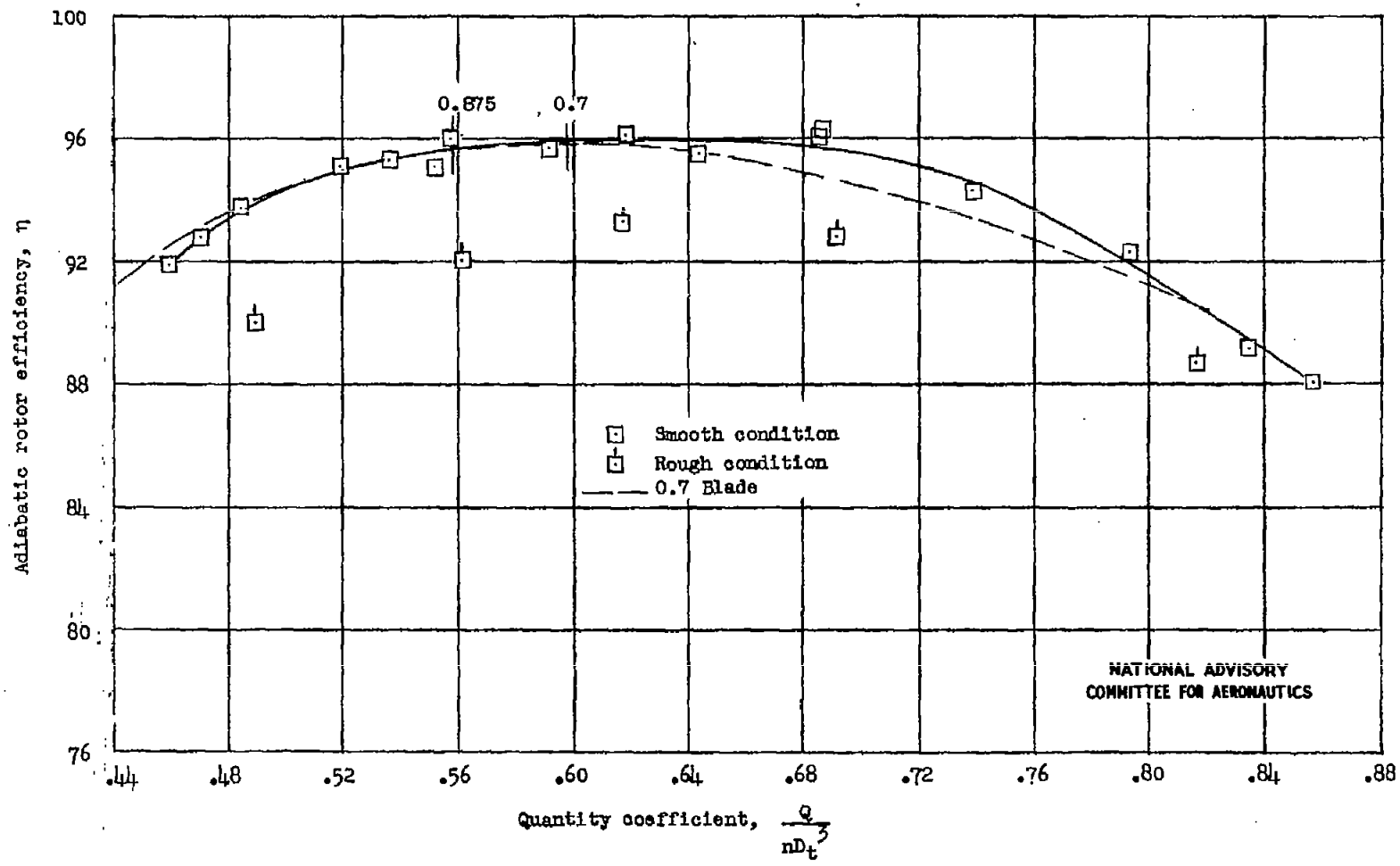

Figure 2.- Variation of efficiency with quantity coefficient for the 0.875 blade in smooth and rough conditions and comparison with results of the 0.7 blade. Efficiency is calculated from surveys and only rotor losses are included. (Short bars across curves are design points.)

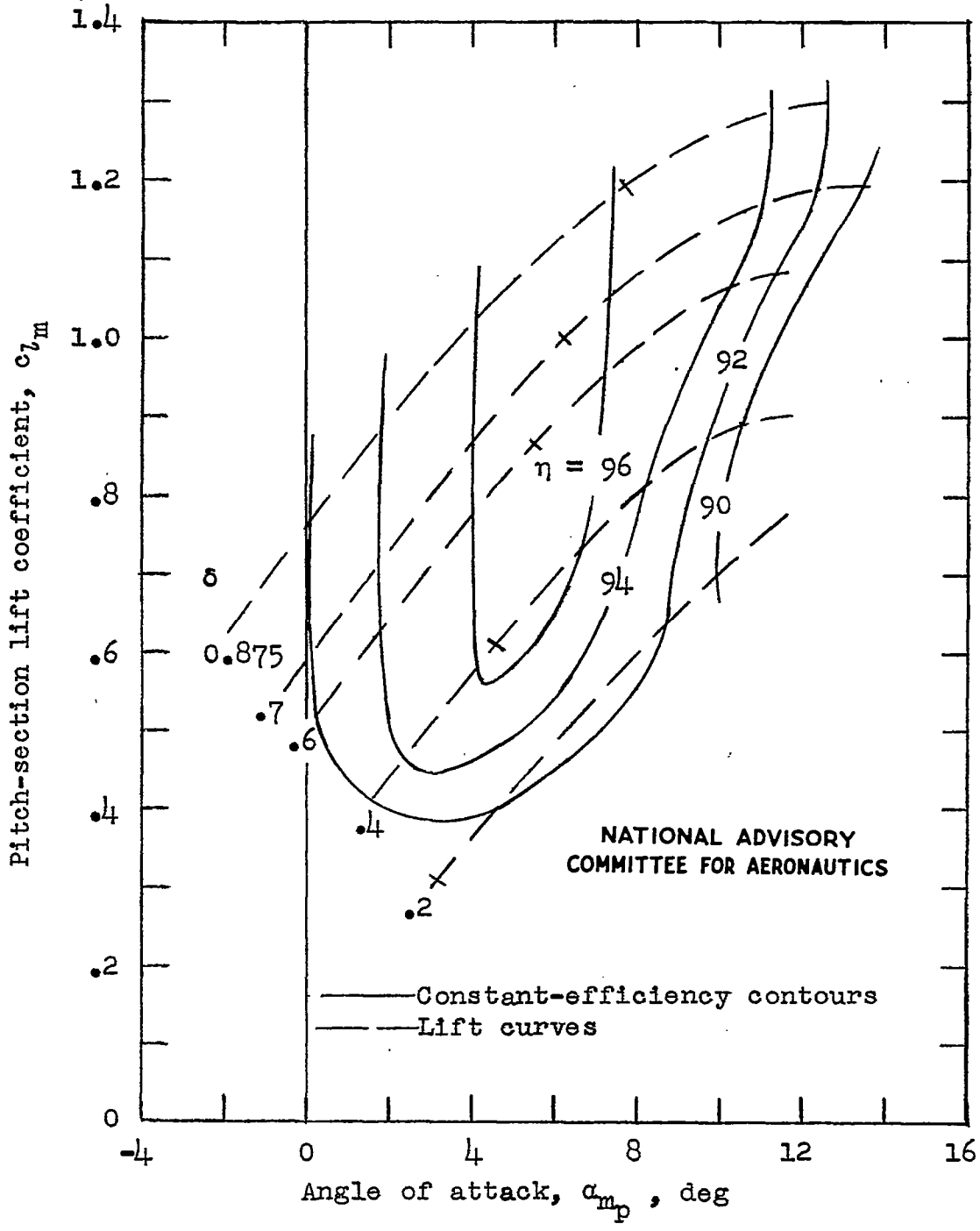

Figure 3.- Measured variation of efficiency with pitch-section lift coefficient. Efficiency is calculated from surveys and only rotor losses are included. (Short bars across curves are design points.)

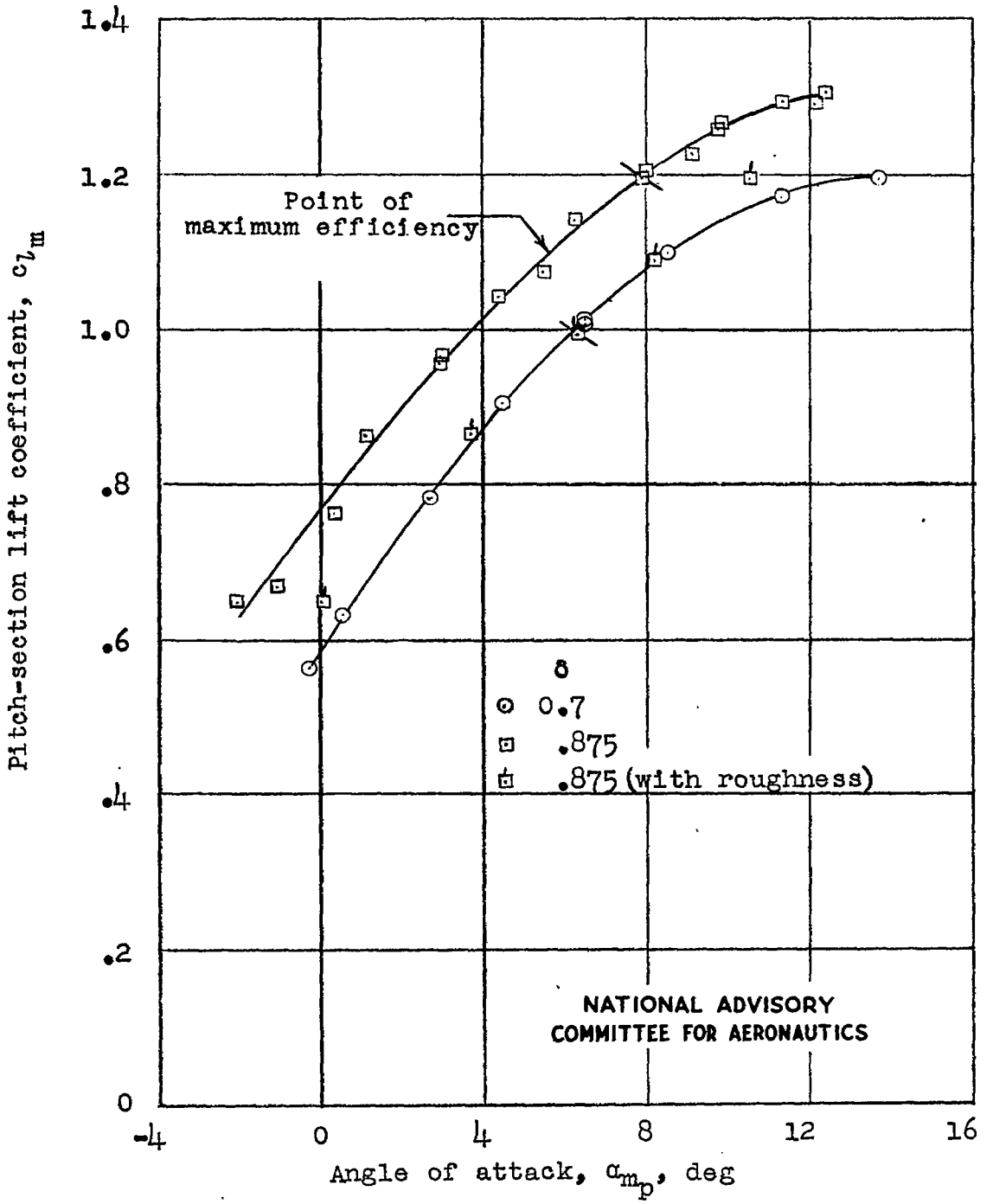

Figure 4.- Comparison of the pitch section lift curve for the 0.875 blade with that for the 0.7 blade. (Short bars across curves are design points.)

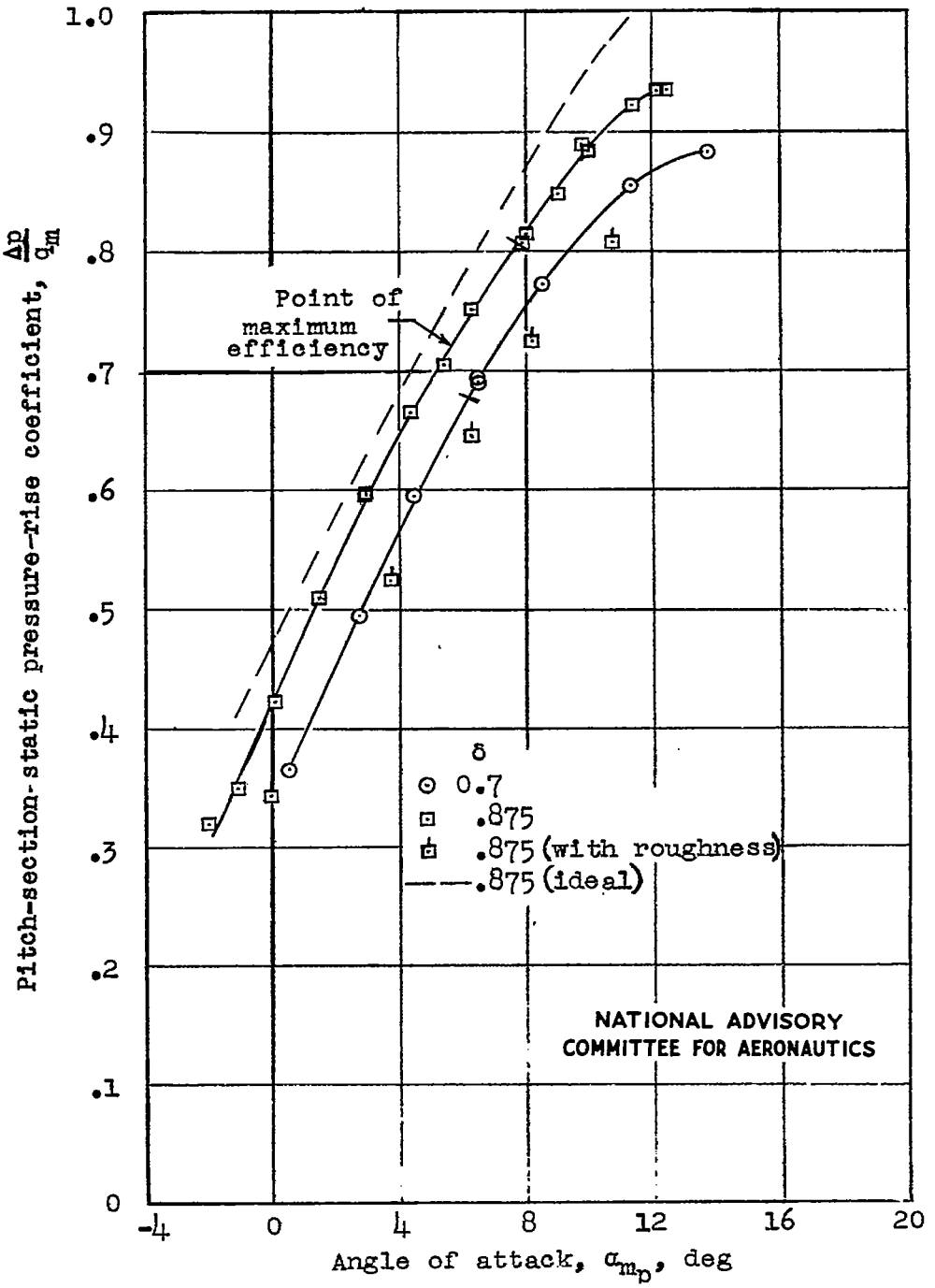

Figure 5.- Comparison of section static-pressure-rise coefficient at the pitch section for the 0.875 and 0.7 blades. (Short bars across curves are design points.)

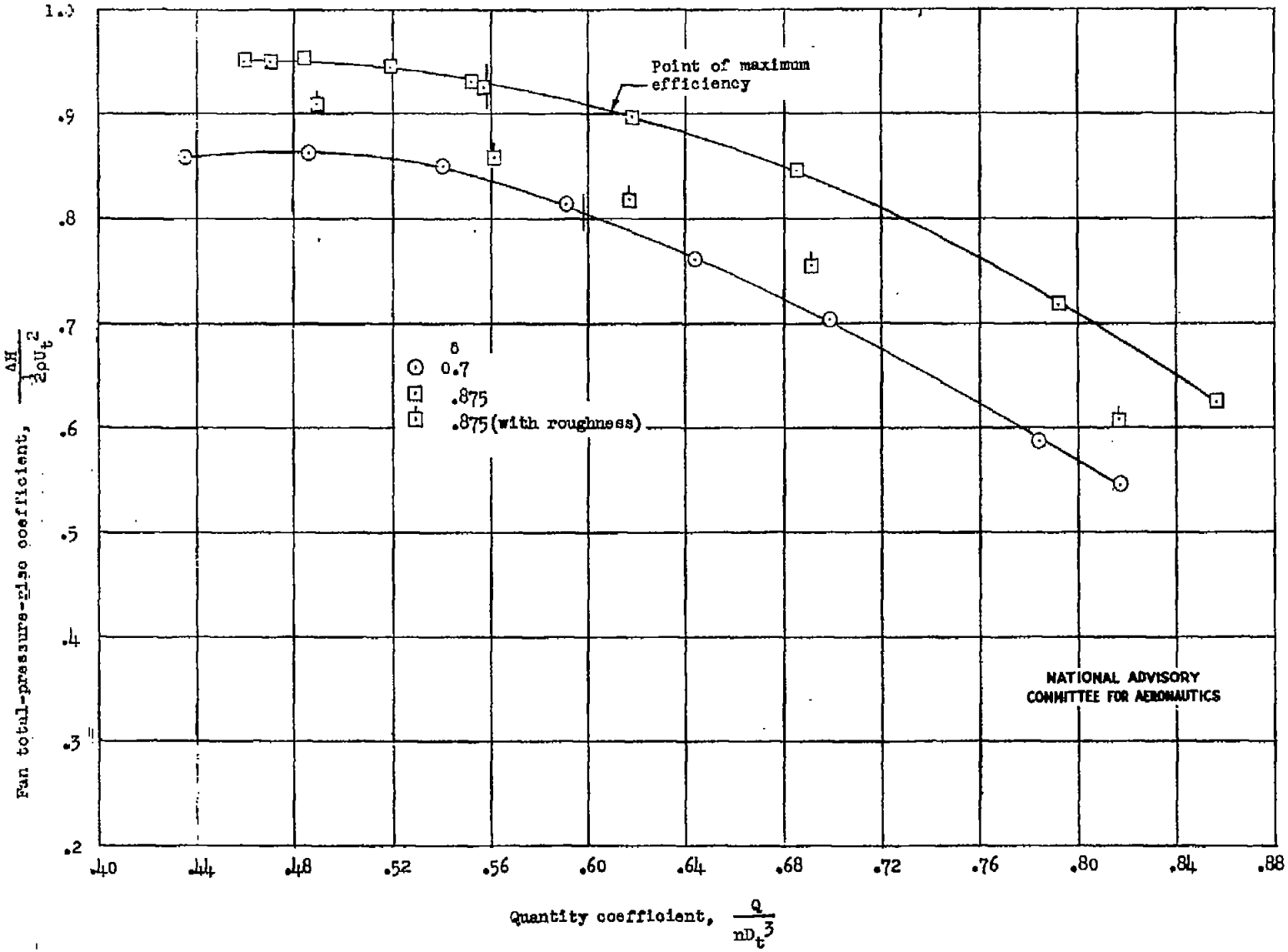

Figure 6.- Comparison of variation of fan weighted-average total-pressure-rise coefficient with quantity coefficient for the 0.875 and 0.7 blades. (Short bars across curves are design points.)

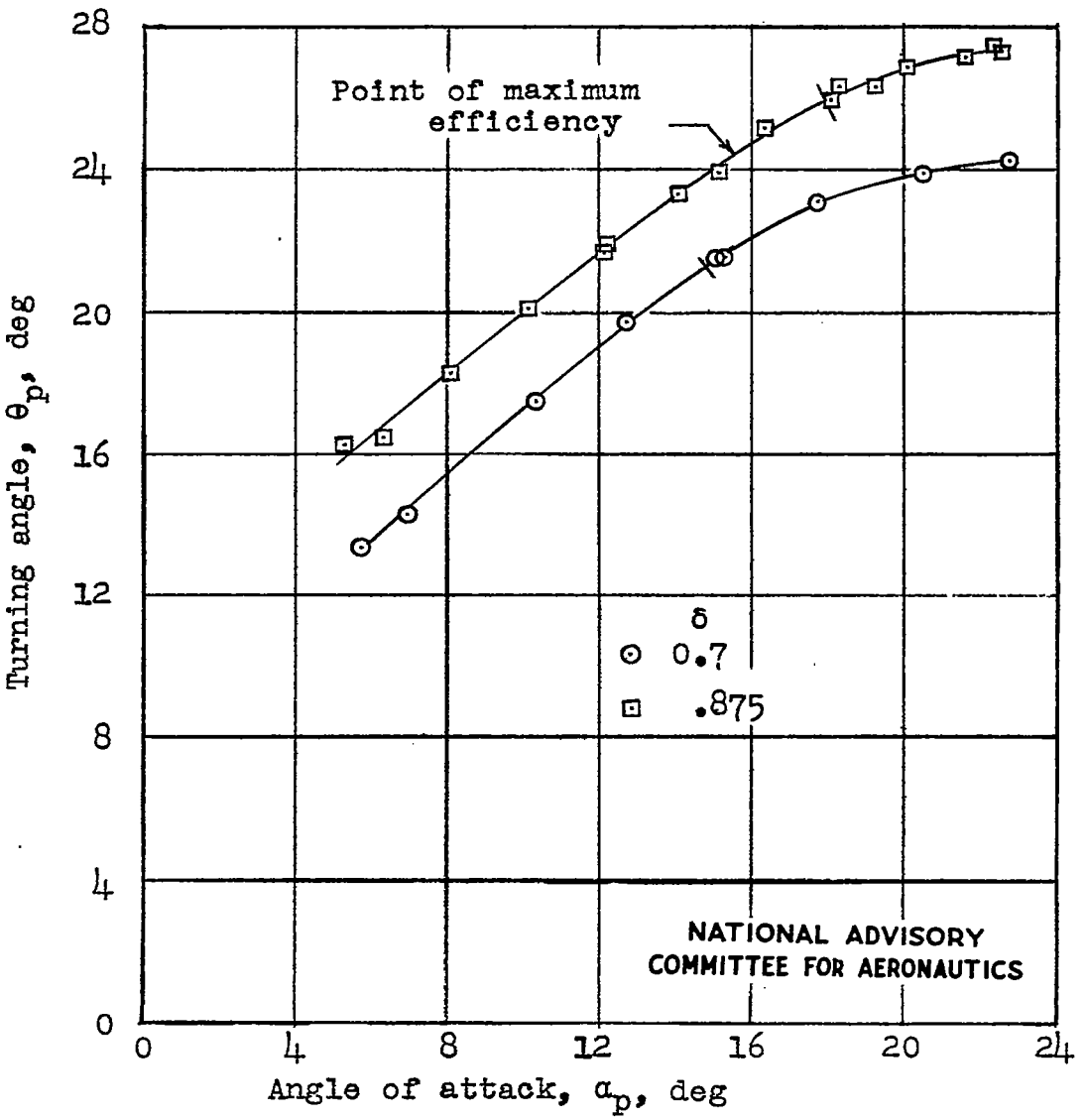

Figure 7.- Comparison of turning angle at the pitch section for the 0.875 and 0.7 blades. (Short bars across curves are design points.)

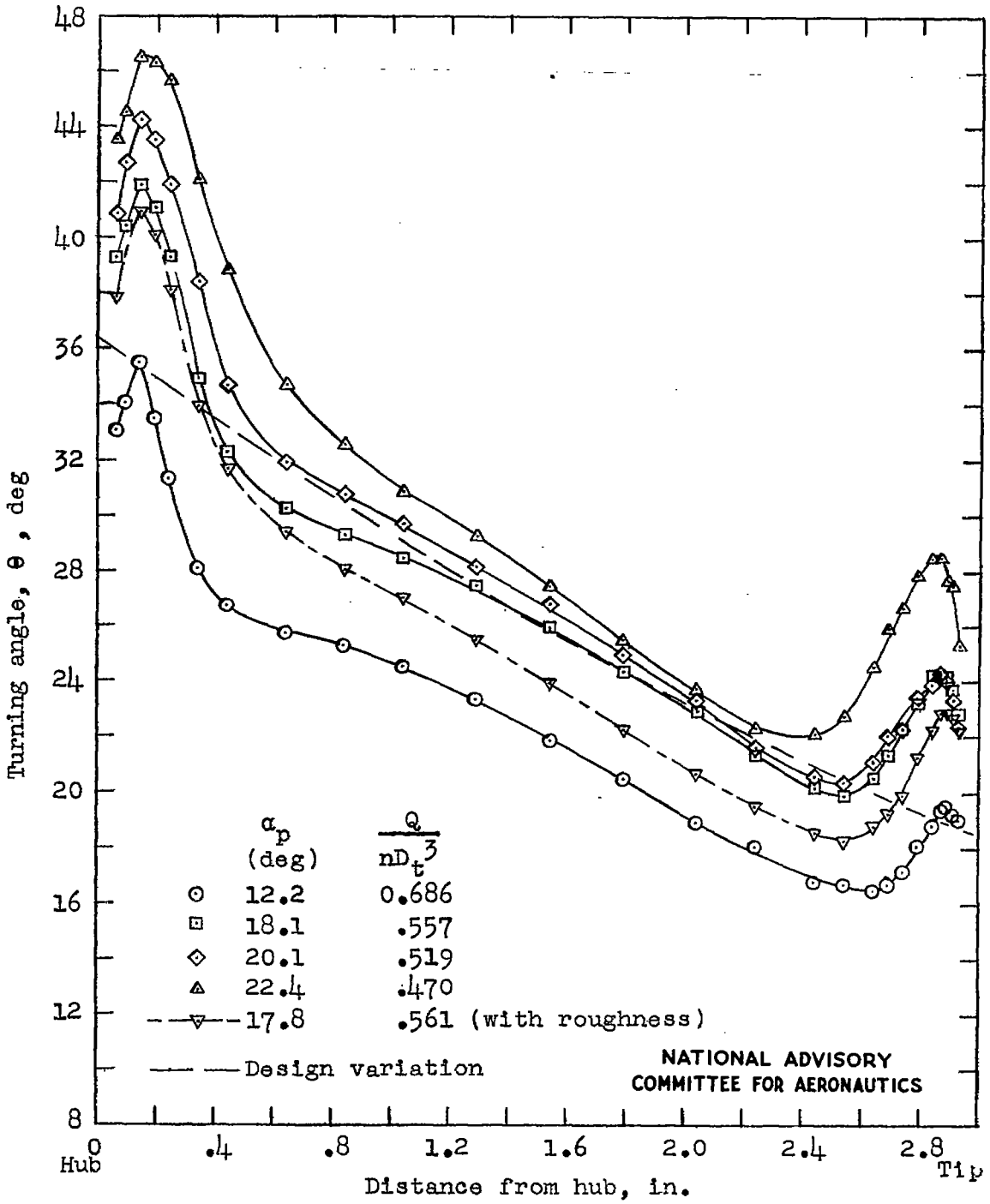

Figure 8.- Variation of turning angle along the 0.875 blade for typical tests. Design conditions: $\alpha_p = 18.0^\circ$; $\frac{Q}{nD_t^3} = 0.558$.

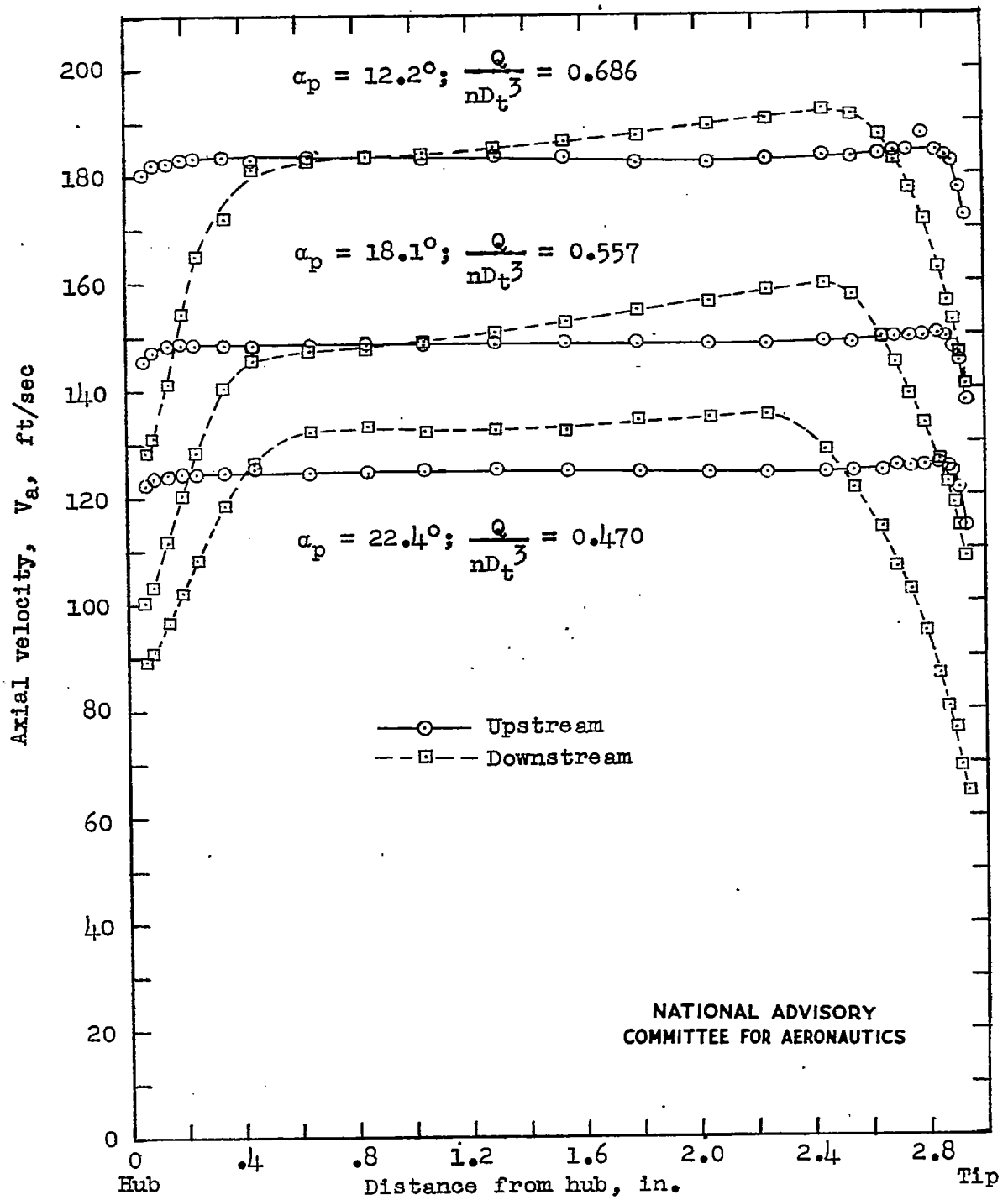

Figure 9.- Axial-velocity surveys at the upstream and downstream survey stations for typical tests. Design conditions: $\alpha_p = 18.0°$; $\frac{Q}{nD_t^3} = 0.558$.

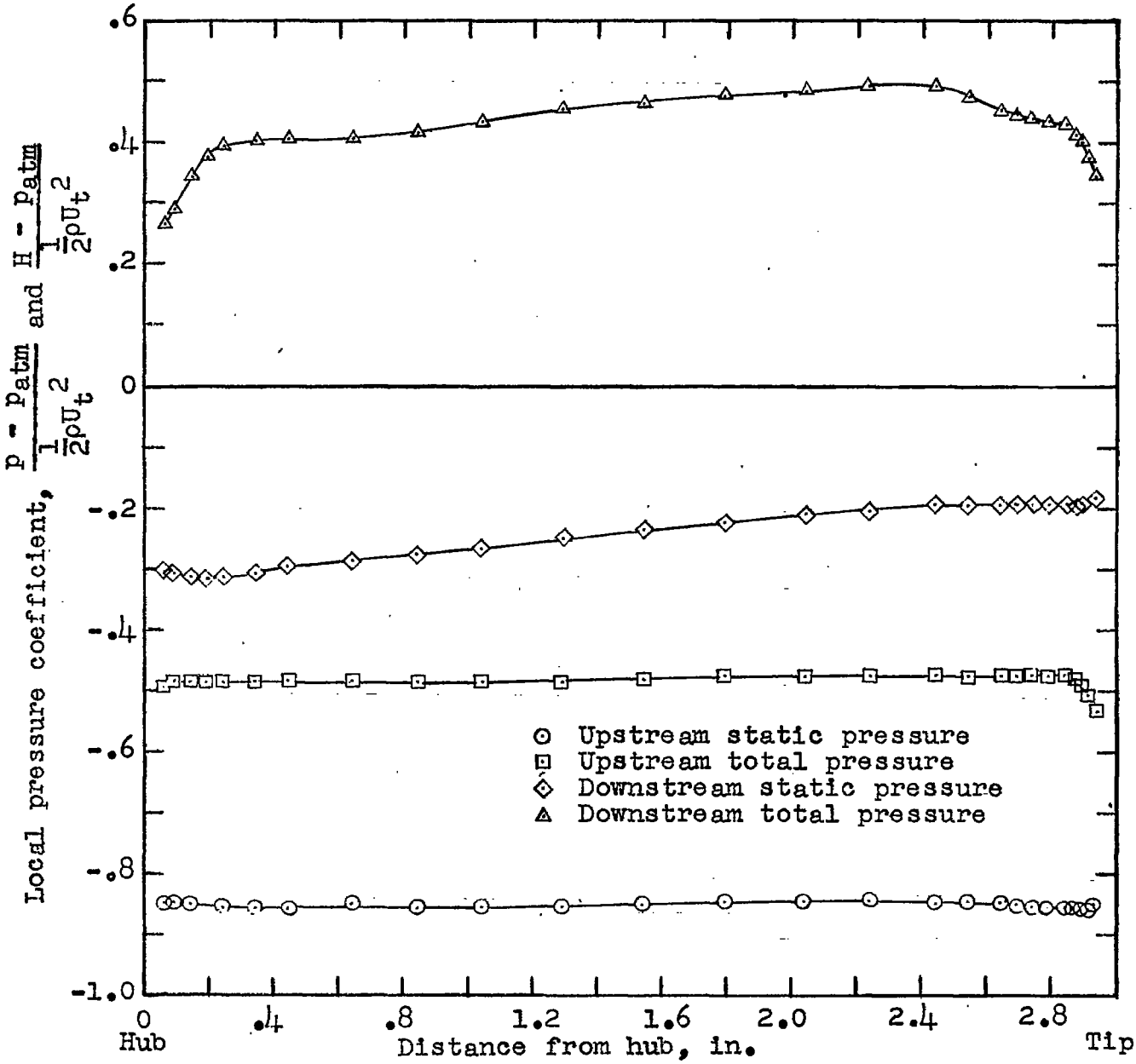

Figure 10.- Typical pressure survey showing variation of static and total pressures along the blade. $\alpha_p = 18.1°$; $\frac{Q}{nD_t^3} = 0.557$.

NATIONAL ADVISORY
COMMITTEE FOR AERONAUTICS